

Anomalous Andreev spectrum and transport in non-Hermitian Josephson junctions

Chang-An Li,^{1,*} Hai-Peng Sun,¹ and Björn Trauzettel^{1,2}

¹*Institute for Theoretical Physics and Astrophysics,
University of Würzburg, 97074 Würzburg, Germany*
²*Würzburg-Dresden Cluster of Excellence ct.qmat, Germany*

(Dated: May 3, 2024)

We propose a phase-biased non-Hermitian Josephson junction (NHJJ) composed of two superconductors mediated by a short non-Hermitian link. Such a NHJJ is described by an effective non-Hermitian Hamiltonian derived based on the Lindblad formalism in the weak coupling regime. By solving the Bogoliubov-de Gennes equation, we find that its Andreev spectrum as a function of phase difference exhibits Josephson gaps, i.e. finite phase windows with no Andreev (quasi-)bound states. The complex Andreev spectrum and the presence of Josephson gaps constitute particular spectral features of the NHJJ. Moreover, we propose complex supercurrents arising from inelastic Cooper pair tunneling to characterize the anomalous transport in the NHJJ. Additional numerical simulations complement our analytical predictions. We demonstrate that the Josephson effect is strongly affected by non-Hermitian physics.

I. INTRODUCTION

In recent years, there has been growing interest in non-Hermitian systems [1–5]. Non-Hermitian physics emerges in a variety of fields such as disordered systems [6, 7], correlated solids [8, 9], and open or driven systems [10–16]. Different from the Hermitian case, the eigenvalues of non-Hermitian systems are complex in general. The complex-valued nature of the spectrum gives rise to unique features such as exceptional points [17–19], point gaps [20, 21], and enriched topological phases [22–25]. Many of these particular phenomena have been theoretically studied and experimentally observed [19–59]. Whereas the research on characterizing novel non-Hermitian systems has achieved impressive progress, the impact of non-Hermiticity on quantum transport is largely unexplored despite some related efforts [60–69], especially for the cases involving superconductivity. For instance, an intriguing open question is how non-Hermiticity affects low-energy spectral features of superconducting systems and results in particular transport signatures.

The best settings to study superconducting transport are Josephson junctions (JJs). Generally, JJs consist of two superconductors separated by a (weak) link [70–73]. Hermitian JJs have been extensively studied for decades. Phase-coherent quantum transport in Hermitian JJs gives rise to the dc Josephson effect: a phase-dependent supercurrent without voltage bias. In the short junction regime, the Josephson effect is entirely determined by the low-energy Andreev spectrum [74–79]. When non-Hermiticity is introduced, we expect that the impact of non-Hermiticity on fundamental properties of JJs, such as the low-energy Andreev spectrum and the phase-biased supercurrent, is substantial. It is also of experimental relevance because JJs are always coupled to the environment and non-Hermitian parts of a Hamiltonian mimic certain aspects of this coupling.

In this work, we investigate the low-energy spec-

trum and transport properties of a short non-Hermitian Josephson junction (NHJJ). The proposed NHJJ is built up of two superconductors connected by a non-Hermitian barrier [Fig. 1(a)]. We discover that the Andreev spectrum becomes complex-valued and exhibits Josephson gaps [purple regions in Fig. 1(b)]. Due to the complex-valued nature of the Andreev spectrum, the supercurrent becomes complex. Its imaginary part signifies the loss of quasiparticles due to inelastic Cooper pair tunneling. We also perform detailed tight-binding calculations to simulate experimental implementations of our proposal.

The article is organized as follows. In Sec. II, we present the construction of the NHJJ and its effective non-Hermitian Hamiltonian from the Lindblad formalism in a weak coupling regime. In Sec. III, we derive the Andreev quasi-bound states and develop the concept of Josephson gaps. In Sec. IV, we present the inelastic Cooper pair tunneling and its consequent complex supercurrents. In Sec. V, we consider the experimental feasibility and numerical simulations of the NHJJ. Finally, we conclude in Sec. VI.

II. EFFECTIVE NON-HERMITIAN HAMILTONIAN OF THE NON-HERMITIAN JOSEPHSON JUNCTIONS

We consider a minimal model of a one-dimensional (1D) NHJJ as sketched in Fig. 1(a). The junction is assumed to be coupled to a fermionic environment, constituting an open quantum system. We derive an effective NH Hamiltonian description for this system from the Lindblad formalism under certain approximations [80–84]. The Hamiltonian for the total quantum system is composed of three parts

$$H = H_S + H_E + H_I, \quad (1)$$

where H_S is the system Hamiltonian, describing the JJ without coupling to the environment. The degrees

of freedom in the environment are described by the Hamiltonian H_E . The interaction between system and environment is captured by H_I . The Hamiltonian of the system can be written in its eigenbasis as $H_S = \sum_{n_s} (\varepsilon_{n_s} - \mu_s) C_{n_s}^\dagger C_{n_s}$ with eigenenergy ε_{n_s} and eigenstate $|n_s\rangle$, where $C_{n_s}^\dagger$ (C_{n_s}) denotes creation (annihilation) operators of the system. They refer to the occupation of Andreev quasi-bound states. The fermionic environment is described by the Hamiltonian $H_E = \sum_{n_e} (\varepsilon_{n_e} - \mu_e) C_{n_e}^\dagger C_{n_e}$. We assume that $\mu_e < \mu_s$, i.e. the chemical potential of the environment is smaller than that of the system. We envision that an external reservoir is coupled to the JJ via a quantum dot, cf. Fig. 1(a). The quantum dot works as a monitor of the tunneling particles between system and reservoir, as we elaborate on below. Note that the Hamiltonian H_E describes the degrees of freedom of the external reservoir and the quantum dot. The coupling Hamiltonian is given by $H_I = \sum_{n_e, n_s} V_{es} C_{n_e}^\dagger C_{n_s} + h.c.$. In general, the interaction term can be decomposed as $H_I = \sum_i S_i \otimes E_i$, where S_i (E_i) is an operator acting on the system (the environment). We make a weak coupling assumption, in the sense, that the coupling between system and environment is weaker than the energy gap of Andreev levels.

The Lindblad master equation describes the dynamics of the system in presence of dissipation due to the environment. The Lindblad master equation takes the form [80–84]

$$\frac{d\rho_S}{dt} = -i[H_S, \rho_S] + \sum_m \gamma (\hat{L}_m \rho_S \hat{L}_m^\dagger - \frac{1}{2} \{\hat{L}_m^\dagger \hat{L}_m, \rho_S\}), \quad (2)$$

where ρ_S is the reduced density matrix of the system and \hat{L}_m the Lindblad operator describing the dissipative dynamics (including decoherence and loss processes) occurring at a positive rate γ [81]. We can rewrite Eq. (2) as

$$\frac{d\rho_S}{dt} = -i(H_{\text{eff}} \rho_S - \rho_S H_{\text{eff}}^\dagger) + \sum_m \gamma \hat{L}_m \rho_S \hat{L}_m^\dagger,$$

where $H_{\text{eff}} = H_S - \frac{i}{2} \sum_m \gamma \hat{L}_m^\dagger \hat{L}_m$. Considering $\mu_e < \mu_s$, we assume that the energy modes of the environment coupled to the system are unoccupied [81]. In this case, we have $\hat{L}_m = C_{m_s}$.

The dissipation term $-\frac{i}{2} \sum_m \gamma \hat{L}_m^\dagger \hat{L}_m$ describes continuous loss of coherence and energy of the system to the environment. Without the quantum-jump term [38, 82, 84], we obtain the equation of motion $\frac{d\rho_S}{dt} = -i(H_{\text{eff}} \rho_S - \rho_S H_{\text{eff}}^\dagger)$, which is equivalent to work with an effective non-Hermitian Hamiltonian

$$H_{\text{eff}} = H_S - \frac{i}{2} \sum_m \gamma \hat{L}_m^\dagger \hat{L}_m. \quad (3)$$

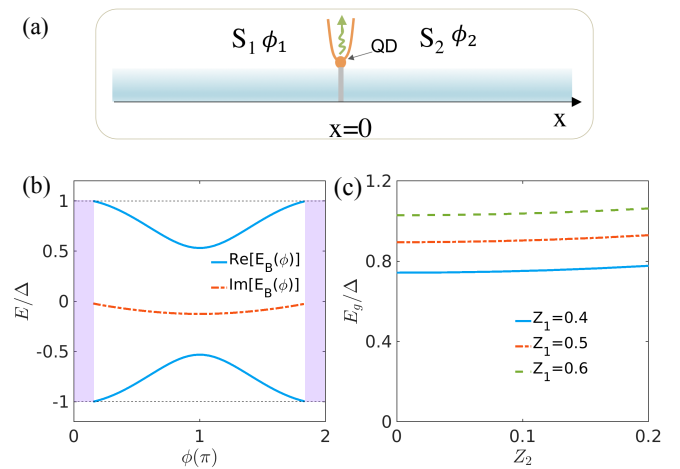


FIG. 1. (a) Sketch of a 1D NHJJ: two superconductors are connected by a short junction, which is coupled to the environment (a reservoir and a quantum dot (QD)). The QD is used to monitor the tunneling of quasiparticles between system and reservoir. The two superconductors possess a phase difference $\phi = \phi_1 - \phi_2$. The wavy line indicates loss due to the coupling to the environment. (b) Complex Andreev spectrum as a function of ϕ within the superconducting gap Δ in the s -wave NHJJ. The purple regions indicate Josephson gaps. We choose $Z_1 = 0.6$ and $Z_2 = 0.2$ here. (c) The energy gap E_g of Andreev spectrum as a function of the parameter Z_2 for different choices of $Z_1 = 0.4, 0.5$ and 0.6 .

The quantum-jump term $\sum_m \gamma \hat{L}_m \rho_S \hat{L}_m^\dagger$ is related to the abrupt change of quantum trajectories [81, 82]. The Lindblad operator takes $\hat{L}_m = C_{m_s}$ in our case. Consider a state $|m_s\rangle = |0, \dots, n_m, \dots\rangle$ in the system H_S . Then the quantum-jump term $\gamma C_{m_s} |m_s\rangle \langle m_s| C_{m_s}^\dagger$ indicates the annihilation of an excitation in the state $|m_s\rangle$. This excitation escapes into the environment. To monitor the quantum-jump process, we assume an auxiliary quantum dot between the junction and the external reservoir, as shown in Fig. 1(a). Note that this setup can be experimentally realized [85]. The quantum dot has a few energy levels. Hence, it is feasible to monitor its occupation e.g. by a nearby quantum point contact. By performing weak measurements and postselection techniques on the quantum dot [86], it is possible to only consider those trajectories where no quantum jumps happen during finite time windows. The average over many such quantum trajectories describes the loss physics due to the dissipation.

To capture this loss physics of the system in a minimal way, we employ a non-Hermitian potential at the junction as $-iV_2 \delta(x)$ with $V_2 > 0$. This non-Hermitian potential mimics the loss of coherence and particles effectively. Furthermore, we assume that the junction between two superconductors also exhibits a real barrier potential described by $V_1 \delta(x)$ with $V_1 > 0$. Hence, we take into account the following scattering potential at

the junction

$$U(x) = (V_1 - iV_2)\delta(x). \quad (4)$$

This gives rise to the effective Hamiltonian $H_{\text{eff}} = H_S + U(x)$.

Explicitly, the Bogoliubov-de Gennes (BdG) Hamiltonian to describe the NHJJ can be written as

$$\mathcal{H}_{\text{BdG}}(x) = \begin{pmatrix} -\frac{\hbar^2 \partial_x^2}{2m} - \mu + U(x) & \hat{\Delta}(x) \\ \hat{\Delta}^\dagger(x) & \frac{\hbar^2 \partial_x^2}{2m} + \mu - U^*(x) \end{pmatrix}, \quad (5)$$

where m is the effective mass of the electrons, μ the chemical potential, and $\hat{\Delta}(x)$ the pairing potential. We argue that the particle-hole symmetry of the type $U\mathcal{H}_{\text{BdG}}^*U^{-1} = -\mathcal{H}_{\text{BdG}}$ is physically relevant in our model (see Appendix A), where U is a unitary matrix. Note that this particle-hole symmetry is labeled as PHS † in the literature [19, 20]. Considering the energy spectrum of the system, electron and hole excitations are described by the BdG equation

$$\mathcal{H}_{\text{BdG}}(x)\psi(x) = E\psi(x), \quad (6)$$

where the eigenstate $\psi(x) = (u(x), v(x))^T$ is a mixture of electron and hole components, and E is the excitation energy measured relative to the Fermi energy. The eigenenergy of \mathcal{H}_{BdG} always comes in pairs $E \longleftrightarrow -E^*$ under PHS † .

III. ANDREEV QUASI-BOUND STATES AND JOSEPHSON GAPS

We consider an s -wave NHJJ, in which the two superconductors are both of s -wave type. Without loss of generality, we assume that left and right superconductors have a constant pairing potential of the same magnitude but different phases, i.e., $\hat{\Delta}(x < 0) = \Delta$ and $\hat{\Delta}(x > 0) = \Delta e^{i\phi}$ where ϕ is the phase difference across the junction. We are interested in the low-energy bound states existing within the superconducting gap. We obtain such Andreev quasi-bound states in the NHJJ by solving the BdG equation with proper boundary conditions. We may write the wave function of bound states as

$$\psi_B(x) = \sum_{\eta, \alpha} A_{\eta\alpha} e^{i\alpha\sigma_\eta k_\eta x} \begin{pmatrix} e^{i\theta_{\eta\alpha}/2} \\ e^{-i\theta_{\eta\alpha}/2} \end{pmatrix}, \quad (7)$$

where $\eta = e/h$, $\sigma_e \equiv 1$, $\sigma_h \equiv -1$, and $\alpha = \pm$. The angles are defined as $\theta_{\eta+} \equiv \sigma_\eta \arccos(E_B/\Delta) + \phi$ and

$\theta_{\eta-} \equiv \sigma_\eta \arccos(E_B/\Delta)$ with the energy of bound states E_B . $A_{\eta\alpha}$ is the coefficient of different evanescent modes. The bound states decay exponentially for $|x| \rightarrow \infty$ with a finite decay length λ . Therefore, the necessary condition for the existence of a bound state is given by $\text{Re}(\lambda) > 0$ with $\lambda = \frac{\hbar v_F}{\Delta} \frac{1}{\sqrt{1 - E_B^2/\Delta^2}}$, where v_F is the Fermi velocity.

A. Andreev quasi-bound states

By considering the boundary conditions of $\psi_B(x)$ at $x = 0$, the secular equation to determine the energy of Andreev quasi-bound state is given by

$$(Z^2 + 1) + 2iZ_2 \sqrt{\frac{\Delta^2}{E_B^2} - 1} = \frac{\Delta^2}{E_B^2} \left(Z^2 + \cos^2 \frac{\phi}{2} \right). \quad (8)$$

The parameter $Z_{j=1,2}$ for the strength of the non-Hermitian barrier potential is defined as $Z_j \equiv \frac{mV_j}{\hbar^2 k_F}$, where k_F is the Fermi wavevector and $Z^2 \equiv \sum_j Z_j^2$.

In the clean case, $Z_1 = Z_2 = 0$, the above equation reduces to the Kulik-Omel'yanchuk (KO) limit $E_B^\pm(\phi) = \pm\Delta \cos \frac{\phi}{2}$ [87]. For $Z_1 \neq 0$ but $Z_2 = 0$, we obtain the known result $E_B^\pm(\phi) = \pm\Delta \sqrt{\frac{Z_1^2 + \cos^2 \frac{\phi}{2}}{Z_1^2 + 1}}$ [74]. In this case, the Andreev spectrum has an energy gap $E_g = \frac{2\Delta Z_1}{\sqrt{Z_1^2 + 1}}$.

Even if the JJ couples weakly to the environment $V_2 \ll E_g$, the imaginary term $2iZ_2 \sqrt{\Delta^2/E_B^2 - 1}$ in Eq. (8) implies a complex Andreev spectrum, different from the Hermitian case [74–79]. The dimensionless parameter Z_2 can be estimated as $Z_2 \sim \frac{V_2 L}{\hbar v_F}$, where V_2 describes the loss rate and L is the junction length. Considering reasonable numbers, Z_2 is estimated to be of the order of $Z_2 \sim 0.1$ [88]. We focus on this experimentally relevant regime of $Z_2 \ll 1$ below.

At special values $\phi = 2n\pi$ with integer n , a trivial solution $E_B^\pm(\phi = 2n\pi) = \pm\Delta$ exists, merging with the continuum. At $\phi = (2n+1)\pi$, we find that the Andreev spectrum becomes

$$E_B^+[(2n+1)\pi] = \frac{Z^2 \Delta}{\sqrt{Z^4 + Z_c^2}}, \quad (9)$$

where $Z_c \equiv Z_1 + iZ_2$ and $E_B^- = -(E_B^+)^*$. The real energy gap E_g obtained from Eq. (9) is illustrated in Fig. 1(c). Evidently, the energy gap E_g is just slightly modified as we turn on a small Z_2 in the weak coupling regime.

For a general phase difference $\phi \in [\phi_b, \phi_t]$, the secular equation can be written as

$$\frac{E^2}{\Delta^2} = \frac{Z^2(Z^2 - \sin^2 \frac{\phi}{2}) + \cos^2 \frac{\phi}{2} + 2Z_1^2 \pm 2Z_2 \sqrt{\cos^2 \frac{\phi}{2}(Z^2 - \sin^2 \frac{\phi}{2}) - Z_1^2}}{(Z^2 + 1)^2 - 4Z_2^2}. \quad (10)$$

We plot the corresponding complex Andreev spectrum obtained from the above equation in Fig. 1(b). The real part of the complex Andreev spectrum indicates the physical energy while its imaginary part characterizes a finite lifetime of quasiparticles traveling across the junction. The phase boundaries are defined as $\phi_b \equiv 2n\pi + \phi_0(Z_2)$ and $\phi_t \equiv (2n+1)\pi - \phi_0(Z_2)$ with $\phi_0(Z_2) \equiv 2 \arcsin(\sqrt{2}Z_2/\sqrt{1+Z^2})$ obtained from the condition $\text{Re}(\lambda) > 0$. For $Z_2 \ll 1$, this phase boundary can be approximated by $\phi_0(Z_2) \simeq \frac{2\sqrt{2}Z_2}{\sqrt{1+Z^2}}$.

B. Josephson gaps

In general, the Andreev spectrum is a continuous function with respect to the phase difference ϕ . However, we find that within a finite phase window $\Phi_W \equiv [2n\pi - \phi_0(Z_2), 2n\pi + \phi_0(Z_2)]$ with $n \in \mathbb{Z}$, low-energy Andreev quasi-bound states are not allowed at all within the superconducting gap Δ . We call such phase windows Josephson gaps. Its gap value is $2\phi_0(Z_2) = 4 \arcsin(\sqrt{2}Z_2/\sqrt{1+Z^2})$. The appearance of Josephson gaps can be understood as a consequence of the competition between phase-coherent transport of Cooper pairs across the junction and decoherence induced by the NH barrier. This competition can be understood by comparing the phase difference ϕ with the loss parameter Z_2 . In the Hermitian case, due to phase coherence across the junction, quasiparticles move back and forth in the junction carrying the phase factor of superconductors imprinted by Andreev reflection [72–74, 89]. Andreev reflections lead to phase-coherent transport of Cooper pairs across the junction, i.e. dc supercurrent. However, the NH mechanism in the NHJJ gives rise to loss of coherence and inelastic Andreev reflections [see Fig. 2(a)] [81, 82, 89]. The magnitude of Z_2 determines the strength of decoherence. Hence, it is clear that the larger Z_2 , the stronger is the coupling between system and environment. For phase differences $\phi \sim 0 \pmod{2\pi}$ associated with a small supercurrent meaning a small number of transferred Cooper pairs, we observe Josephson gaps. This implies that phase-coherent transport of Cooper pairs is totally absent (thus no bound states). For larger supercurrents, i.e. larger phase differences, the pair breaking mechanism related to the barrier strength Z_2 is not sufficient to block the supercurrent. Nevertheless, decoherence modifies the supercurrent in this case. The Josephson-gap phase boundary $\phi_0(Z_2)$ depends on the value of Z_2 . In Fig. 2(b), we plot the Josephson-gap phase boundary as a function of Z_2 . It grows almost

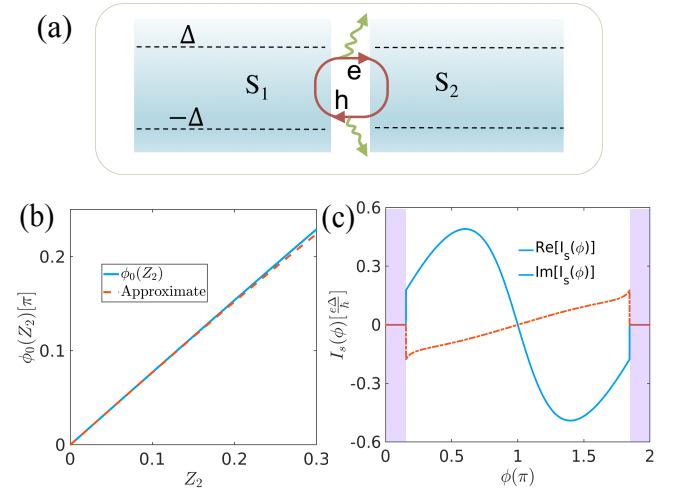


FIG. 2. (a) Sketch of inelastic Cooper pair tunneling. Transfer of Cooper pairs experiences possible decoherence and quasiparticles loss (wavy lines). (b) Josephson-gap phase boundary $\phi_0(Z_2)$ as a function of Z_2 . (c) Complex supercurrents as a function of ϕ with $Z_1 = 0.6$ and $Z_2 = 0.2$.

linearly with increasing Z_2 .

IV. INELASTIC COOPER PAIR TUNNELING AND COMPLEX SUPERCURRENT

In (short) Hermitian JJs, the supercurrent originates from the coherent Cooper pair tunneling related to the Andreev spectrum [71, 74, 90]. In NHJJs, the Andreev spectrum becomes complex. The imaginary part of the Andreev spectrum indicates a finite lifetime of quasiparticles. Thus, the NH mechanism introduces loss of quasiparticles and decoherence during the Andreev reflection processes [80–82, 89] [see Fig. 2(a)], leading to inelastic Cooper pair tunneling [91–95].

The supercurrent $I_s(\phi)$ can be obtained by taking the derivative of the free energy with respect to the phase difference ϕ [71]. It leads to $I_s(\phi) = -\frac{2e}{\hbar} \sum_{n>0} \frac{dE_n(\phi)}{d\phi}$ with the Andreev spectrum $E_n(\phi)$ in Hermitian JJs [71, 90]. In NHJJ, the real part of the Andreev spectrum is the physical energy while the imaginary part corresponds to a finite lifetime of each eigenstate. The free energy in the ground state of NHJJs can be interpreted as the summation of real energy levels, broadened due to imaginary parts up to the Fermi energy [38]. Following the same reasoning as in Hermitian JJs, we derive the supercurrent as

$$I_s(\phi) = -\frac{2e}{\hbar} \frac{d\text{Re}[E_B^+(\phi)]}{d\phi} + i \frac{2e}{\hbar} \frac{d\text{Im}[E_B^+(\phi)]}{d\phi}, \quad (11)$$

where $E_B^+(\phi)$ is the complex Andreev spectrum. The real part $\text{Re}[I_s(\phi)]$ represents the physical supercurrent flowing across JJs. The imaginary part $\text{Im}[I_s(\phi)]$ stems from phase-dependent lifetimes of quasiparticles during inelastic Cooper pair tunneling. Thus, it is associated with the loss of quasiparticles from the JJ to the environment [96]. Indeed, it is possible for either electrons or holes to escape the JJs after experiencing inelastic scattering at the NH barrier. If we consider scattering of electrons or holes, the scattering probability becomes $P(E, Z_1, Z_2) < 1$, which means that some quasiparticles escape into the environment from the JJ (see Appendix B).

Explicitly for *s*-wave NHJJs, within the phase region $\phi \in [\phi_b, \phi_t]$, the supercurrent as a function of ϕ is plotted in Fig. 2(c). Within the Josephson gaps, there is no supercurrent flowing across the junction. The supercurrent exhibits a jump at the phase boundary $\phi_0(Z_2)$. We note that imaginary currents in normal states have been employed to describe delocalized behavior or dissipation of eigenstates [97–99], while to the best of our knowledge, a complex supercurrent has not been addressed before.

V. EXPERIMENTAL CONSIDERATIONS AND NUMERICAL SIMULATIONS

Our analysis of NHJJs is experimentally relevant, considering the advanced fabrication techniques of JJs. The *s*-wave JJs could, for instance, be built by aluminum-based or InAs-based superconductor nanowires [100–102]. The local loss at the junction may stem from the coupling of JJs to the environment with a dissipative lead [103, 104]. In the following, we provide more evidence from numerical simulations.

To perform tight-binding calculations, we discretize the Hamiltonian on a one-dimensional lattice by the long-wavelength approximation. The lattice constant is set at $a = 1$. We divide the system to three parts: the left side and the right side are superconductors of length L_s , the middle region is the normal part of length L_N . To mimic the loss at the junction, we set $L_N = 1a$ and an on-site complex potential $V_1 - iV_2$. The two superconductors have a paring potential Δ and a phase difference ϕ .

Figure 3(a) shows the real part of the Andreev spectra as a function of ϕ for the NHJJ. Note the presence of the Josephson gap. Figure 3(b) illustrates the real part of the supercurrent obtained from the Andreev spectra corresponding to Fig. 3(a). The supercurrent vanishes within the Josephson gap.

To evaluate the phase boundary $\phi_0(Z_2)$, we need the estimate Z_j via $Z_j = \frac{mV_j}{\hbar^2 k_F}$. The phase boundary is

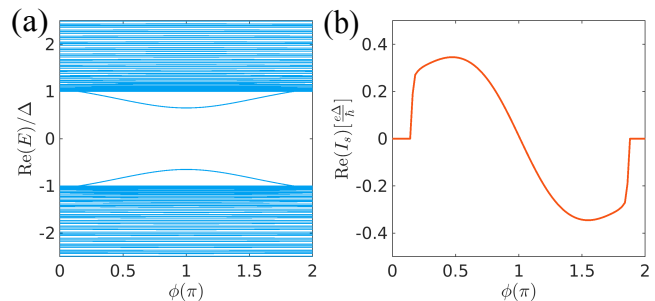


FIG. 3. Tight-binding simulations of the *s*-wave NHJJ with a finite length. (a) Real part of energy spectra as a function of ϕ . (b) Real supercurrent as a function of ϕ obtained from corresponding energy spectra in panel (a). We choose $V_1 = 0.8$, $V_2 = 0.3$, $\mu = 1$, and $L_s = 100a$ here.

then obtained as $\phi_0(Z_2) = 2 \arcsin \left(\frac{\sqrt{2}Z_2}{\sqrt{1+Z^2}} \right)$. For the parameters used in Fig. 3(b), we obtain $Z_1 = 0.566$, and $Z_2 = 0.212$, which gives $\phi_0(Z_2) = 0.165\pi$, in accordance with the plot.

VI. DISCUSSION AND CONCLUSIONS

To summarize, we have studied the low-energy spectral features and transport properties of NHJJs. Our minimal model of NHJJs reveals anomalous NH physics emerging in JJs. We have introduced several conceptually new phenomena, including Josephson gaps and complex supercurrents, with no counterparts in the Hermitian case.

Our work extends the realm of the Josephson effect to NH physics and inspires potential applications: the NHJJ may function as a supercurrent switch by tuning the phase difference ϕ exploiting the presence of Josephson gaps. The impact of non-Hermiticity on other related phenomena, such as ac Josephson effects, Shapiro steps [73], JJ circuits [105], and Josephson diode effects [106], are interesting extensions of our work.

VII. ACKNOWLEDGMENTS

We thank Jan Budich, Haiping Hu, Jian Li, Zhuo-Yu Xian, and Chunxu Zhang for valuable discussions. This work was supported by the Würzburg-Dresden Cluster of Excellence ct.qmat, EXC2147, project-id 390858490, the DFG (SFB 1170), and the Bavarian Ministry of Economic Affairs, Regional Development and Energy within the High-Tech Agenda Project “Bausteine für das Quanten Computing auf Basis topologischer Materialien”.

Note added.—Recently, we came to notice a related work on NHJJs [107].

Appendix A: Relevant particle-hole symmetry of the model

In this section, we analyze the particle-hole symmetry that is physically relevant from a general form. From a field operator perspective, the particle-hole symmetry (PHS) mixes creation operator Ψ^\dagger and annihilation operator Ψ in a way

$$C\Psi_\alpha C^{-1} = U_{\alpha\beta}\Psi_\beta^\dagger, \quad C\Psi_\alpha^\dagger C^{-1} = \Psi_\alpha U_{\alpha\beta}^T, \quad (\text{A1})$$

where U represents a unitary matrix and C denotes the PHS operator. A Hamiltonian $H = \Psi_\alpha^\dagger \mathcal{H}_{\alpha\beta} \Psi_\beta$ is particle-hole symmetric if $CHC^{-1} = H$. This implies that the first-quantized Hamiltonian transforms under PHS as

$$C\mathcal{H}^T C^{-1} = -\mathcal{H}, \quad (\text{A2})$$

where T is the transpose operation. In the Hermitian case, $\mathcal{H}^T = \mathcal{H}^*$. While in the non-Hermitian case, $\mathcal{H}^T \neq \mathcal{H}^*$ in general. Thus, the PHS comes in two kinds as [19]:

$$\begin{aligned} U\mathcal{H}^*U^{-1} &= -\mathcal{H}, \text{ type I;} \\ U\mathcal{H}^TU^{-1} &= -\mathcal{H}, \text{ type II.} \end{aligned} \quad (\text{A3})$$

In the presence of PHS, the excitation energy of \mathcal{H} always comes in pairs. For the two types of PHSs above, the corresponding energy pairs are $E \longleftrightarrow -E^*$ for type I PHS and $E \longleftrightarrow -E$ for type II PHS, respectively.

To determine which one of the two types of PHS on \mathcal{H} is physically more relevant, we further consider the constraint of PHS on Green's functions. On the one hand, the effective Hamiltonian \mathcal{H} is directly related with the retarded Green's function. Note that the poles of the retarded Green's function yield the eigenvalues of the Hamiltonian, located in the lower half of the complex plane. On the other hand, the physical indication of the retarded Green's function as a propagator is consistent with causality. The retarded Green's function is defined in terms of field operators as $G_{\alpha\beta}^R(t) = -i\theta(t)\langle[\Psi_\alpha(t), \Psi_\beta^\dagger(0)]\rangle$, where t is the time domain and $\theta(t)$ is a Heaviside step function. Considering PHS on

field operators in Green's function, it leads to

$$\begin{aligned} G_{\alpha\beta}^R(t) &= -i\theta(t)\langle[\Psi_\alpha(t), \Psi_\beta^\dagger(0)]\rangle \\ &= -i\theta(t)\langle C^{-1}C[\Psi_\alpha(t), \Psi_\beta^\dagger(0)]\rangle \\ &= -i\theta(t)\langle C[\Psi_\alpha(t), \Psi_\beta^\dagger(0)]C^{-1}\rangle \\ &= -U_{\alpha\gamma}^*\langle i\theta(t)[\Psi_\gamma^\dagger(0), \Psi_\delta(-t)]\rangle U_{\delta\beta}^T \\ &= -U_{\alpha\gamma}^*G_{\gamma\delta}^A(-t)U_{\delta\beta}^T. \end{aligned} \quad (\text{A4})$$

By Fourier transformation and relating the retarded and advanced Green's function by $[G_{\alpha\beta}^R(E)]^* = G_{\alpha\beta}^A(E)$, the retarded Green's function fulfills

$$U^\dagger[G^R(E)]^*U = -G^R(-E). \quad (\text{A5})$$

This PHS constraint on retarded Green's function is consistent with type I PHS acting on \mathcal{H} : The eigenvalues of the system (poles of the Green's function) reside on the same side of the complex plane $\text{Im}[E] \leq 0$. In contrast, from the constraint of type II PHS acting on \mathcal{H} , eigenvalues distribute symmetrically in the upper and lower half of the complex plane. This symmetric eigenenergy distribution is not consistent with the eigenvalues obtained from the retarded Green's function. Thus, it is not compatible with the requirement of causality. Therefore, we argue that type I PHS acting on \mathcal{H} is physically more relevant to describe non-Hermitian systems. This type I PHS is employed in the main text and labeled as PHS^\dagger .

Appendix B: Quasiparticle loss due to non-Hermitian barrier scattering

In this section, we obtain the reflection amplitudes (Andreev reflection and the normal reflection) and tunneling amplitudes (crossed Andreev tunneling and the normal tunneling) of quasiparticles after scattering at the non-Hermitian barrier. We show explicitly the loss of quasiparticles from the junction to the environment due to non-Hermitian scatterings. Consider an electron-like quasiparticle that is propagating from the left side of the junction. The wave function can be written as

$$\psi(x) = \begin{pmatrix} u(x) \\ v(x) \end{pmatrix} = \begin{cases} e^{ik_e x} \begin{pmatrix} u_0 \\ v_0 \end{pmatrix} + A_{h-}e^{ik_h x} \begin{pmatrix} v_0 \\ u_0 \end{pmatrix} + A_{e-}e^{-ik_e x} \begin{pmatrix} u_0 \\ v_0 \end{pmatrix}, & x < 0; \\ A_{e+}e^{ik_e x} \begin{pmatrix} u_0 e^{i\phi/2} \\ v_0 e^{-i\phi/2} \end{pmatrix} + A_{h+}e^{-ik_h x} \begin{pmatrix} v_0 e^{i\phi/2} \\ u_0 e^{-i\phi/2} \end{pmatrix}, & x > 0. \end{cases} \quad (\text{B1})$$

Note that $u_0^2 = \frac{1}{2} \left(1 + i\frac{\sqrt{\Delta^2 - E^2}}{E}\right)$, $v_0^2 = \frac{1}{2} \left(1 - i\frac{\sqrt{\Delta^2 - E^2}}{E}\right)$. The wave vectors are defined as $\hbar k_e = \sqrt{2m(\mu + i\sqrt{\Delta^2 - E^2})}$, $k_h = k_e^*$. The coefficients are determined by the boundary conditions:

$$\psi(0+) = \psi(0-), \quad (B2)$$

$$\psi'(0+) - \psi'(0-) = \frac{2m}{\hbar^2} (V_1 \tau_0 - i V_2 \tau_z) \psi(0+). \quad (B3)$$

By solving these linear equations, the four coefficients (Andreev reflection A_{h-} , normal reflection A_{e-} , normal tunneling A_{e+} , crossed Andreev tunneling A_{h+}) are obtained as

$$A_{h-} = -\frac{\Delta [E \sin^2 \frac{\phi}{2} + \Omega(i \sin \frac{\phi}{2} \cos \frac{\phi}{2} - Z_2)]}{(Z^2 + 1)E^2 + 2Z_2 \Omega E - \Delta^2(Z^2 + \cos^2 \frac{\phi}{2})}, \quad (B4)$$

$$A_{e-} = -\frac{Z^2 \Omega^2 - Z_2 \Omega E - i Z_1 \Omega^2}{(Z^2 + 1)E^2 + 2Z_2 \Omega E - \Delta^2(Z^2 + \cos^2 \frac{\phi}{2})}, \quad (B5)$$

$$A_{e+} = -\frac{\Omega E [Z_2 \cos \frac{\phi}{2} + i(1 + iZ_1) \sin \frac{\phi}{2}] - \Omega^2 [(1 + iZ_1) \cos \frac{\phi}{2} + iZ_2 \sin \frac{\phi}{2}]}{(Z^2 + 1)E^2 + 2Z_2 \Omega E - \Delta^2(Z^2 + \cos^2 \frac{\phi}{2})}, \quad (B6)$$

$$A_{h+} = \frac{\Delta \Omega [Z_2 \cos \frac{\phi}{2} - Z_1 \sin \frac{\phi}{2}]}{(Z^2 + 1)E^2 + 2Z_2 \Omega E - \Delta^2(Z^2 + \cos^2 \frac{\phi}{2})}. \quad (B7)$$

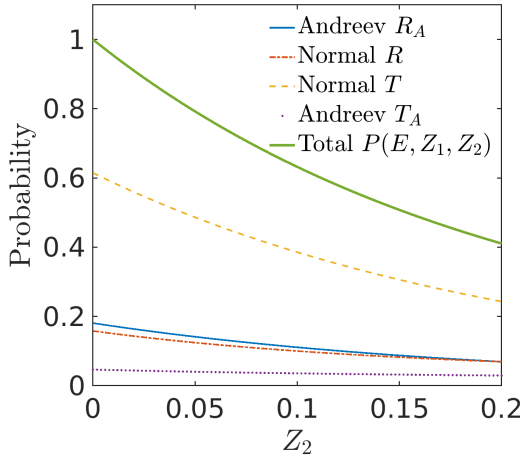


FIG. 4. Scattering probabilities as a function of Z_2 for fixed $Z_1 = 0.6$. We chose $\phi = \frac{\pi}{2}$ in this plot. We choose $E = 1.5$ in unit of Δ .

The parameter Ω is defined as $\Omega \equiv \sqrt{E^2 - \Delta^2}$. The total scattering probability is defined as

$$P(E, Z_1, Z_2) = \sum_{\eta=e/h, s=\pm} |A_{\eta s}|^2. \quad (B8)$$

In the Hermitian case, the probability is conserved at $P(E, Z_1, Z_2 = 0) = 1$. For nonzero Z_2 , we find that the probability $P(E, Z_1, Z_2) < 1$, which indicates the loss of quasiparticles from the junction to the environment [as shown in Figs. 4(a) and 4(b)]. The probability $P(E, Z_1, Z_2)$ decays continuously as increasing the

strength of Z_2 . Thus, the value of Z_2 measures the magnitude of loss.

-
- * changan.li@uni-wuerzburg.de
- [1] C. M. Bender, Rep. Prog. Phys. **70**, 947 (2007).
 - [2] R. El-Ganainy, K. G. Makris, M. Khajavikhan, Z. H. Musslimani, S. Rotter, and D. N. Christodoulides, Nat. Phys. **14**, 11 (2018).
 - [3] Y. Ashida, Z. Gong, and M. Ueda, Adv. Phys. **69**, 249 (2020).
 - [4] E. J. Bergholtz, J. C. Budich, and F. K. Kunst, Rev. Mod. Phys. **93**, 015005 (2021).
 - [5] N. Okuma and M. Sato, Ann. Rev. Condens. Matter Phys. **14**, 83 (2023).
 - [6] A. A. Zyuzin and A. Y. Zyuzin, Phys. Rev. B **97**, 041203 (2018).
 - [7] M. Papaj, H. Isobe, and L. Fu, Phys. Rev. B **99**, 201107 (2019).
 - [8] T. Yoshida, R. Peters, N. Kawakami, and Y. Hatsugai, Phys. Rev. B **99**, 121101 (2019).
 - [9] Y. Nagai, Y. Qi, H. Isobe, V. Kozii, and L. Fu, Phys. Rev. Lett. **125**, 227204 (2020).
 - [10] K. G. Makris, R. El-Ganainy, D. N. Christodoulides, and Z. H. Musslimani, Phys. Rev. Lett. **100**, 103904 (2008).
 - [11] A. Guo, G. J. Salamo, D. Duchesne, R. Morandotti, M. Volatier-Ravat, V. Aimez, G. A. Siviloglou, and D. N. Christodoulides, Phys. Rev. Lett. **103**, 093902 (2009).
 - [12] I. Rotter, J. Phys. A: Math. Theor. **42**, 153001 (2009).
 - [13] M. Nakagawa, N. Kawakami, and M. Ueda, Phys. Rev. Lett. **121**, 203001 (2018).
 - [14] L. Xiao, K. Wang, X. Zhan, Z. Bian, K. Kawabata,

- M. Ueda, W. Yi, and P. Xue, Phys. Rev. Lett. **123**, 230401 (2019).
- [15] J. Li, A. K. Harter, J. Liu, L. de Melo, Y. N. Joglekar, and L. Luo, Nat. Commun. **10**, 855 (2019).
- [16] X. Zhang and J. Gong, Phys. Rev. B **101**, 045415 (2020).
- [17] C. Dembowski, H.-D. Gräf, H. L. Harney, A. Heine, W. D. Heiss, H. Rehfeld, and A. Richter, Phys. Rev. Lett. **86**, 787 (2001).
- [18] M. V. Berry, Czechoslovak Journal of Physics **54**, 1039 (2004).
- [19] K. Kawabata, T. Bessho, and M. Sato, Phys. Rev. Lett. **123**, 066405 (2019).
- [20] K. Kawabata, K. Shiozaki, M. Ueda, and M. Sato, Phys. Rev. X **9**, 041015 (2019).
- [21] H. Zhou and J. Y. Lee, Phys. Rev. B **99**, 235112 (2019).
- [22] T. E. Lee, Phys. Rev. Lett. **116**, 133903 (2016).
- [23] S. Yao and Z. Wang, Phys. Rev. Lett. **121**, 086803 (2018).
- [24] F. K. Kunst, E. Edvardsson, J. C. Budich, and E. J. Bergholtz, Phys. Rev. Lett. **121**, 026808 (2018).
- [25] Z. Gong, Y. Ashida, K. Kawabata, K. Takasan, S. Higashikawa, and M. Ueda, Phys. Rev. X **8**, 031079 (2018).
- [26] K. Zhang, Z. Yang, and C. Fang, Phys. Rev. Lett. **125**, 126402 (2020).
- [27] N. Okuma, K. Kawabata, K. Shiozaki, and M. Sato, Phys. Rev. Lett. **124**, 086801 (2020).
- [28] S. Yao, F. Song, and Z. Wang, Phys. Rev. Lett. **121**, 136802 (2018).
- [29] Q.-B. Zeng, B. Zhu, S. Chen, L. You, and R. Lü, Phys. Rev. A **94**, 022119 (2016).
- [30] P. San-Jose, J. Cayao, E. Prada, and R. Aguado, Scientific Reports **6**, 21427 (2016).
- [31] D. Leykam, K. Y. Bliokh, C. Huang, Y. D. Chong, and F. Nori, Phys. Rev. Lett. **118**, 040401 (2017).
- [32] H. Shen, B. Zhen, and L. Fu, Phys. Rev. Lett. **120**, 146402 (2018).
- [33] C. Yin, H. Jiang, L. Li, R. Lü, and S. Chen, Phys. Rev. A **97**, 052115 (2018).
- [34] K. Yokomizo and S. Murakami, Phys. Rev. Lett. **123**, 066404 (2019).
- [35] C. H. Lee and R. Thomale, Phys. Rev. B **99**, 201103 (2019).
- [36] S. Longhi, Phys. Rev. Lett. **122**, 237601 (2019).
- [37] J. Y. Lee, J. Ahn, H. Zhou, and A. Vishwanath, Phys. Rev. Lett. **123**, 206404 (2019).
- [38] K. Yamamoto, M. Nakagawa, K. Adachi, K. Takasan, M. Ueda, and N. Kawakami, Phys. Rev. Lett. **123**, 123601 (2019).
- [39] J. Avila, F. Peñaranda, E. Prada, P. San-Jose, and R. Aguado, Communications Physics **2**, 133 (2019).
- [40] D. S. Borgnia, A. J. Kruchkov, and R.-J. Slager, Phys. Rev. Lett. **124**, 056802 (2020).
- [41] J. C. Budich and E. J. Bergholtz, Phys. Rev. Lett. **125**, 180403 (2020).
- [42] K. Yamamoto, M. Nakagawa, N. Tsuji, M. Ueda, and N. Kawakami, Phys. Rev. Lett. **127**, 055301 (2021).
- [43] S. Franca, V. Könye, F. Hassler, J. van den Brink, and C. Fulga, Phys. Rev. Lett. **129**, 086601 (2022).
- [44] J. Cayao and A. M. Black-Schaffer, Phys. Rev. B **105**, 094502 (2022).
- [45] L. Jezequel and P. Delplace, Phys. Rev. Lett. **130**, 066601 (2023).
- [46] F. Qin, R. Shen, and C. H. Lee, Phys. Rev. A **107**, L010202 (2023).
- [47] C.-X. Guo, S. Chen, K. Ding, and H. Hu, Phys. Rev. Lett. **130**, 157201 (2023).
- [48] J. Cayao and A. M. Black-Schaffer, Phys. Rev. B **107**, 104515 (2023).
- [49] J. Sun, C.-A. Li, S. Feng, and H. Guo, Phys. Rev. B **108**, 075122 (2023).
- [50] C.-A. Li, B. Trauzettel, T. Neupert, and S.-B. Zhang, Phys. Rev. Lett. **131**, 116601 (2023).
- [51] V. Kornich, Phys. Rev. Lett. **131**, 116001 (2023).
- [52] J. M. Zeuner, M. C. Rechtsman, Y. Plotnik, Y. Lumer, S. Nolte, M. S. Rudner, M. Segev, and A. Szameit, Phys. Rev. Lett. **115**, 040402 (2015).
- [53] K. Ding, G. Ma, M. Xiao, Z. Q. Zhang, and C. T. Chan, Phys. Rev. X **6**, 021007 (2016).
- [54] L. Xiao, T. Deng, K. Wang, G. Zhu, Z. Wang, W. Yi, and P. Xue, Nature Physics **16**, 761 (2020).
- [55] F. E. Ozturk, T. Lappe, G. Hellmann, J. Schmitt, J. Klaers, F. Vewinger, J. Kroha, and M. Weitz, Science **372**, 88 (2021).
- [56] Q. Liang, D. Xie, Z. Dong, H. Li, H. Li, B. Gadway, W. Yi, and B. Yan, Phys. Rev. Lett. **129**, 070401 (2022).
- [57] Q. Zhang, Y. Li, H. Sun, X. Liu, L. Zhao, X. Feng, X. Fan, and C. Qiu, Phys. Rev. Lett. **130**, 017201 (2023).
- [58] C. Liang, Y. Tang, A.-N. Xu, and Y.-C. Liu, Phys. Rev. Lett. **130**, 263601 (2023).
- [59] G. Xu, X. Zhou, Y. Li, Q. Cao, W. Chen, Y. Xiao, L. Yang, and C.-W. Qiu, Phys. Rev. Lett. **130**, 266303 (2023).
- [60] B. Zhu, R. Lü, and S. Chen, Phys. Rev. A **93**, 032129 (2016).
- [61] S. Longhi, Phys. Rev. B **95**, 014201 (2017).
- [62] Y. Chen and H. Zhai, Phys. Rev. B **98**, 245130 (2018).
- [63] E. J. Bergholtz and J. C. Budich, Phys. Rev. Res. **1**, 012003 (2019).
- [64] K. Shobe, K. Kuramoto, K.-I. Imura, and N. Hatano, Phys. Rev. Res. **3**, 013223 (2021).
- [65] B. Michen and J. C. Budich, Phys. Rev. Res. **4**, 023248 (2022).
- [66] V. Kornich and B. Trauzettel, Phys. Rev. Res. **4**, 033201 (2022).
- [67] D. Sticlet, B. Dóra, and C. P. Moca, Phys. Rev. Lett. **128**, 016802 (2022).
- [68] H. Geng, J. Y. Wei, M. H. Zou, L. Sheng, W. Chen, and D. Y. Xing, Phys. Rev. B **107**, 035306 (2023).
- [69] H. Isobe and N. Nagaosa, Phys. Rev. B **107**, L201116 (2023).
- [70] K. K. Likharev, Rev. Mod. Phys. **51**, 101 (1979).
- [71] C. W. J. Beenakker, in *Transport Phenomena in Mesoscopic Systems*, edited by H. Fukuyama and T. Ando (Springer Berlin Heidelberg, Berlin, Heidelberg, 1992) pp. 235–253.
- [72] A. A. Golubov, M. Y. Kupriyanov, and E. Il'ichev, Rev. Mod. Phys. **76**, 411 (2004).
- [73] M. Tinkham, *Introduction to Superconductivity* (Dover Publications, Inc., Garden City, New York, 1996).
- [74] A. Furusaki, Superlattices Microst. **25**, 809 (1999).
- [75] C. W. J. Beenakker and H. van Houten, Phys. Rev. Lett. **66**, 3056 (1991).
- [76] H.-J. Kwon, K. Sengupta, and V. M. Yakovenko, Eur. Phys. J. B **37**, 349 (2004).

- [77] L. Fu and C. L. Kane, Phys. Rev. B **79**, 161408 (2009).
- [78] F. Dolcini, M. Houzet, and J. S. Meyer, Phys. Rev. B **92**, 035428 (2015).
- [79] C. W. J. Beenakker, D. I. Pikulin, T. Hyart, H. Schomerus, and J. P. Dahlhaus, Phys. Rev. Lett. **110**, 017003 (2013).
- [80] H. P. Breuer and F. Petruccione, *The theory of open quantum systems* (Oxford University Press, Great Clarendon Street, 2002).
- [81] A. J. Daley, Advances in Physics **63**, 77 (2014).
- [82] F. Minganti, A. Miranowicz, R. W. Chhajlany, and F. Nori, Phys. Rev. A **100**, 062131 (2019).
- [83] D. Manzano, AIP Advances **10**, 025106 (2020).
- [84] F. Roccati, G. M. Palma, F. Ciccarello, and F. Bagarello, Open Syst. Inf. Dyn. **29**, 2250004 (2022).
- [85] M. T. Deng, S. Vaitiekėnas, E. B. Hansen, J. Danon, M. Leijnse, K. Flensberg, J. Nygård, P. Krogstrup, and C. M. Marcus, Science **354**, 1557 (2016).
- [86] M. Naghiloo, M. Abbasi, Y. N. Joglekar, and K. W. Murch, Nature Physics **15**, 1232 (2019).
- [87] I. O. Kulik and A. N. Omel'yanchuk, JETP Lett. **21**, 96 (1975).
- [88] If we assume $V_2 \sim 1$ meV (a typical energy scale of our setup), junction length $L \sim 100$ nm, and Fermi velocity $v_F \sim 1 \times 10^6$ m/s, the parameter Z_2 can be estimated as $Z_2 \sim \frac{V_2 L}{\hbar v_F} \approx 0.1$. The value of Z_2 can in principle be tuned by junction length L and loss rate V_2 by changing the coupling between JJ and environment.
- [89] Y. V. Nazarov and Y. M. Blanter, *Quantum Transport: Introduction to Nanoscience* (Cambridge University Press, 2006).
- [90] C. W. J. Beenakker, Phys. Rev. Lett. **67**, 3836 (1991).
- [91] M. H. Devoret, D. Esteve, H. Grabert, G.-L. Ingold, H. Pothier, and C. Urbina, Phys. Rev. Lett. **64**, 1824 (1990).
- [92] G.-L. Ingold and Y. V. Nazarov, in *Single charge tunneling: Coulom Blockade Phenomena in Nanostructures*, edited by H. Gruber and M. H. Devoret (Plenum, Neeew York, 1994) p. 21.
- [93] M. Hofheinz, F. Portier, Q. Baudouin, P. Joyez, D. Vion, P. Bertet, P. Roche, and D. Esteve, Phys. Rev. Lett. **106**, 217005 (2011).
- [94] M. Westig, B. Kubala, O. Parlavecchio, Y. Mukharsky, C. Altimiras, P. Joyez, D. Vion, P. Roche, D. Esteve, M. Hofheinz, M. Trif, P. Simon, J. Ankerhold, and F. Portier, Phys. Rev. Lett. **119**, 137001 (2017).
- [95] A. Grimm, F. Blanchet, R. Albert, J. Leppäkangas, S. Jebari, D. Hazra, F. Gustavo, J.-L. Thomassin, E. Dupont-Ferrier, F. Portier, and M. Hofheinz, Phys. Rev. X **9**, 021016 (2019).
- [96] The lifetime of quasiparticles becomes phase dependent. Thus, the magnitude of imaginary supercurrent indicates the response of quasiparticles loss as changing ϕ .
- [97] N. Hatano and D. R. Nelson, Phys. Rev. Lett. **77**, 570 (1996).
- [98] S.-B. Zhang, M. M. Denner, T. Bzdušek, M. A. Sentef, and T. Neupert, Phys. Rev. B **106**, L121102 (2022).
- [99] Q. Li, J.-J. Liu, and Y.-T. Zhang, Phys. Rev. B **103**, 035415 (2021).
- [100] Y.-J. Doh, J. A. van Dam, A. L. Roest, E. P. A. M. Bakkers, L. P. Kouwenhoven, and S. De Franceschi, Science **309**, 272 (2005).
- [101] W. Chang, S. M. Albrecht, T. S. Jespersen, F. Kuemmeth, P. Krogstrup, J. Nygård, and C. M. Marcus, Nature Nanotechnology **10**, 232 (2015).
- [102] M. Hays, G. de Lange, K. Serniak, D. J. van Woerkom, D. Bouman, P. Krogstrup, J. Nygård, A. Geresdi, and M. H. Devoret, Phys. Rev. Lett. **121**, 047001 (2018).
- [103] S. Zhang, Z. Wang, D. Pan, H. Li, S. Lu, Z. Li, G. Zhang, D. Liu, Z. Cao, L. Liu, L. Wen, D. Liao, R. Zhuo, R. Shang, D. E. Liu, J. Zhao, and H. Zhang, Phys. Rev. Lett. **128**, 076803 (2022).
- [104] D. Liu, G. Zhang, Z. Cao, H. Zhang, and D. E. Liu, Phys. Rev. Lett. **128**, 076802 (2022).
- [105] M. H. Devoret and R. J. Schoelkopf, Science **339**, 1169 (2013).
- [106] F. Ando, Y. Miyasaka, T. Li, J. Ishizuka, T. Arakawa, Y. Shiota, T. Moriyama, Y. Yanase, and T. Ono, Nature **584**, 373 (2020).
- [107] J. Cayao and M. Sato, (2023), arXiv:2307.15472 [cond-mat.supr-con].